Hindawi Publishing Corporation
Shock and Vibration
Volume 2015, Article ID 294980, 10 pages
http://dx.doi.org/10.1155/2015/294980

Research Article

Vibration Characteristics Induced by Cavitation in a Centrifugal Pump with Slope Volute

Ning Zhang, Minguan Yang, Bo Gao, and Zhong Li

School of Energy and Power Engineering, Jiangsu University, Zhenjiang 212013, China

Correspondence should be addressed to Ning Zhang; zhangningwlg@163.com

Received 4 May 2014; Accepted 13 August 2014

Academic Editor: Vadim V. Silberschmidt

Cavitation is one of the instability sources in centrifugal pump, which would cause some unexpected results. The goal of this paper was to analyze the influence of cavitation process on different frequency bands in a centrifugal pump with slope volute. And special attention was paid to low frequency signals, which were often filtered in the reported researches. Results show that at noncavitation condition, vibration level is closely related to flow structure interior pump. At partial flow rates, especially low flow rates, vibration level increases rapidly with the onset of rotating stall. At cavitation condition, it is proved that cavitation process has a significant impact on low frequency signals. With cavitation number decreasing, vibration level first rises to a local maximum, then it drops to a local minimum, and finally it rises again. At different flow rates, vibration trends in variable frequency bands differ obviously. Critical point inferred from vibration level is much larger than that from 3% head drop, which indicates that cavitation occurs much earlier than that reflected in head curve. Also, it is noted that high frequency signals almost increase simultaneously with cavitation occurring, which can be used to detect cavitation in centrifugal pump.

1. Introduction

Cavitation is one of the main problems which should be considered seriously in designing and operating a centrifugal pump. At some extreme conditions, cavitation may cause huge damage to impeller [1]. Cavitation occurs when absolute static pressure at some location of impeller, usually at blade leading edge, falls below the vapor pressure of fluid at the prevailing temperature [2]. The number and size of cavitation bubbles increase with net positive suction head (NPSH) decreasing. Cavitation bubbles travel to impeller downstream with the flow; when they move to a high pressure area they collapse intensively. Shock waves, forces are generated during collapse process. If the implosion position is near solid wall, cavitation erosion phenomenon may easily occur. So it is essential to detect and avoid cavitation developing in centrifugal pump.

Many methods could be used to identify cavitation in centrifugal pump: vibration and noise measurement of model pump; visualization of flow field interior impeller channels; determination of head drop. The most common method used to detect presence of cavitation in centrifugal pump is to identify the drop of head. Net positive suction head in accordance with 3% drop of total delivery head is usually defined as $NPSH_c$ (critical point), and cavitation is considered full developed under this working condition. But it is noted that cavitation inception starts to develop much earlier before usual critical point [3].

Cavitation interior centrifugal pump would cause many unexpected consequences: noise, vibration, and cavitation erosion [4]. Many researches have been done to investigate vibration and noise induced by cavitation in hydraulic machineries [5]. Christopher and Kumaraswamy [6] used noise and vibration signals to identify critical net positive suction head in a radial flow pump. And critical NPSH inferred from 3% head drop was compared with from noise and vibration spectra, and the difference was analyzed. Rus et al. [7] analyzed relationship between noise, vibration, acoustic emission, and cavitation structure using measurement and visualization methods on a Kaplan Turbine. Vibration energy trend versus various NPSH was presented in the paper and a model was established to predict cavitation noise.

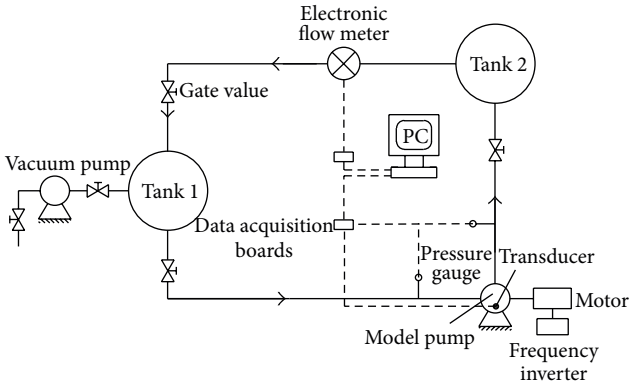

Figure 1: Test platform.

Table 1: Measuring direction of accelerometer.

Accelerometer	Position	Measuring direction
Sensor 1	Volute tongue	$-y$
Sensor 2	Volute outlet	$+x, +y, -z$
Sensor 3	The second cross-section of volute	$+x, +y, +z$
Sensor 4	The forth cross-section of volute	$+x$
Sensor 5	Volute inlet	$+x, -y, +z$
Sensor 6	Side surface of the forth cross-section	$+x, -y, +z$
Sensor 7	Side surface of the second cross-section	$+y$

Čudina [8, 9] adopted noise spectra to detect cavitation in a centrifugal pump and found a strong relationship between a discrete frequency 147 Hz and development process of cavitation. Ni et al. [10] used vibration method to detect cavitation in a centrifugal pump, and vibration signals at noncavitation and cavitation conditions were compared. Pearsall [11] investigated cavitation noise and vibration in a centrifugal pump and found fundamental trend of vibration energy. However most of the researches were concerning high frequency signals; low frequency signals were often neglected leading to a lack of comprehensive understanding of vibration characteristics in different frequency bands. According to the work of McNulty and Pearsall [12], low frequency signals below 1 kHz were cut off during vibration signal processing. So a thorough explanation of vibration energy trends in different frequency bands was rarely given in centrifugal pump.

In this paper, a special slope volute was proposed to reduce rotor-stator interaction in centrifugal pump [13]. According to our previous study [14], it has an effective impact on reducing pressure pulsation magnitude. Vibration energy trends in various frequency bands were investigated. This paper attempts to clarify cavitation induced vibration characteristics in a centrifugal pump with slope volute. And an overall understanding of cavitation induced vibration characteristic would be carried out leading to improvement of detecting and controlling cavitation in centrifugal pump.

2. Experimental Setup

Experiments were carried out in a closed-loop test rig to guarantee measuring accuracy of model pump, as seen in Figure 1. Absolute static pressure in cavitation tank 1 was reduced gradually using vacuum pump to lower net positive suction head of model pump. Flow rates of model pump at variable conditions were measured by electronic flowmeter with an absolute accuracy of ±0.2% of measured value. The head of model pump was measured with an uncertainty of less than ±0.1% of the measured value. Flexible joints were fixed at the inlet and outlet of model pump to reduce the influence of interference signals from experimental system on vibration signals of model pump. Several accelerometers were mounted on surface of slope volute to obtain vibration characteristic. And the accelerometer has a flat frequency response from 0.5 Hz to 5 kHz. Meanwhile the typical resonant frequency is about 50 kHz. Rotating speed of model pump at variable flow rates was kept at a constant value 1450 r/min. Figure 2 shows the relative position of impeller in slope volute. It is found that conventional spiral volute tongue directly faces the impeller; however, slope volute tongue locates at the right side of impeller. The diffusion section of slope volute has an acute angle of about 15° with vertical axis based on optimal results [13]. Radial size along volute periphery keeps constant, while the cross-section area of volute increases along axis direction.

3. Measuring Schemes

LMS vibration measurement systems were applied to acquire vibration signal by placing accelerometers at typical positions of slope volute surface. LMS vibration test systems are widely used in vibration test field, which support dynamic signal sampling by using 24 sampling channels. And the maximum sampling frequency of each channel almost reaches 102.4 kHz. Seven accelerometers were mounted on the surface of slope volute to have an overall understanding of vibration characteristics. Figure 3 shows the positions of accelerometers, and measuring direction of each sensor is presented in Table 1.

During signal sampling process, rotating speed kept constant at different flow rates, and sampling frequency was set as 80 kHz to satisfy Nyquist sampling theorem [15]. So the sampled signal could keep detailed information of original signal. Sampling resolution was set as 1 Hz, and sampling time was set to 3 s. Meanwhile, sampling interval was 0.5 s. Haning window was employed to reduce vibration energy leakage during sampling process. And the time domain signals were transformed into frequency domain signals using auto-power spectrum algorithm.

4. Results of Measurements

4.1. Results at Noncavitation Condition. A centrifugal pump with slope volute was first designed. The main parameters of model pump are presented in Table 2.

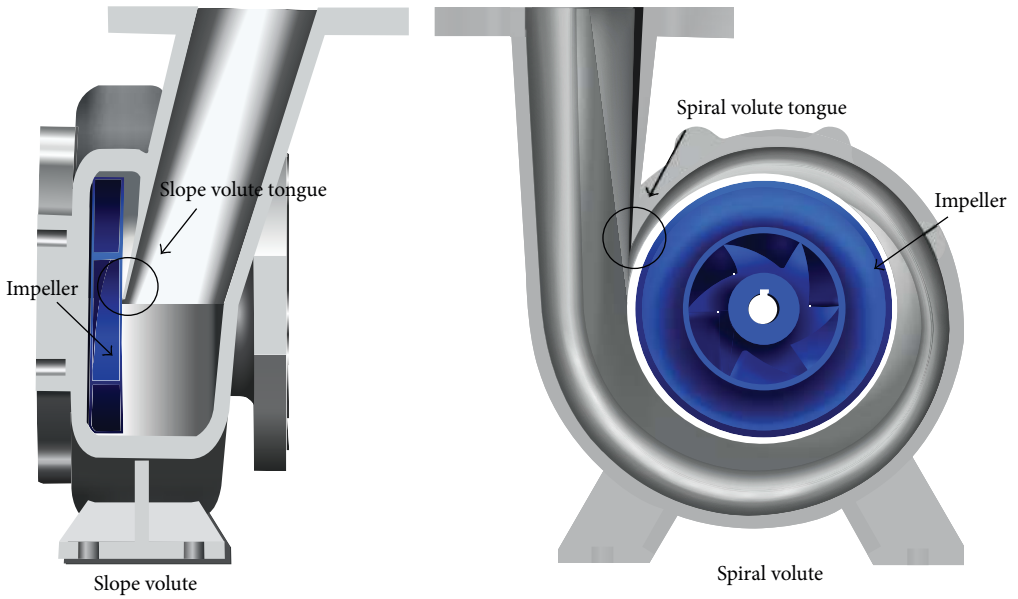

Figure 2: Comparison of slope volute and conventional spiral volute.

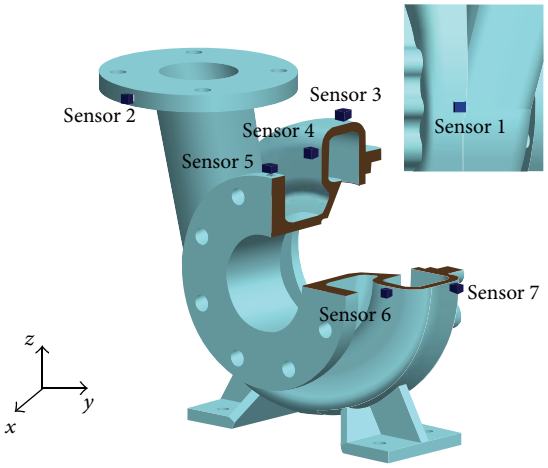

Figure 3: Position of accelerometer.

Table 2: Main parameters of model pump.

Parameters	Value
Nominal flow rate Q_N	48 m^3/h
Designed head H_N	7.5 m
Rotating speed n	1450 r/min
Impeller inlet diameter d_j	100 mm
Impeller outlet diameter d_2	172 mm
Impeller outlet width b_2	17 mm
Blade number Z	6
Nominal flow rate coefficient Φ_N	$Q_N/(\omega {d_2}^2 b_2)$
Nominal head coefficient Ψ_N	$gH_N/(\omega^2 {d_2}^2)$
Shaft power coefficient λ	$P/{d_2}^5 n^3$

Experimental performance results of model pump were carried out from shutoff condition to $1.45\Phi_N$ as shown in Figure 4. The best efficiency point of model pump is around designed flow rate $1.0\Phi_N$. At low flow rates, positive slope (hump phenomenon) occurs in head curve of model pump, which indicates that rotating stall phenomenon develops interior impeller channels under these working conditions [16].

Vibration experiments of model pump were conducted at different flow rates. Vibration signals in 0–10 Hz were filtered. Root mean square (RMS) method [17] was used to deal with acceleration signals as shown in

$$\mathrm{RMS} = \sqrt{\frac{1}{n}\sum_{n=1}^{n}\left(A_n - \overline{A}\right)^2}, \tag{1}$$

where A_n represents acceleration amplitudes at different frequencies, and $\overline{A}$ is mean amplitude:

$$\overline{A} = \frac{1}{n}\sum_{n=1}^{n} A_n. \tag{2}$$

For triaxial accelerometer, total vibration energy E was used to evalute vibration energy at different measurinig directions. And it is defined as shown in

$$E = \sqrt{\frac{\mathrm{RMS}_x^2 + \mathrm{RMS}_y^2 + \mathrm{RMS}_z^2}{3}}. \tag{3}$$

Many researches have proved that hydraulic factors mainly cause low frequency vibration signals. So vibration signals in low frequency band (10–500 Hz) of slope volute pump were used to analyze vibration energy characteristic

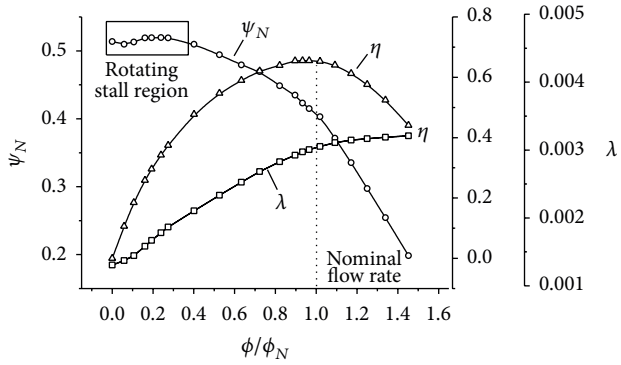

Figure 4: Performance of model pump.

versus flow rate. Flow rate of model pump was first divided into four typical regions: region I (0–0.3Φ_N), region II (0.3Φ_N–0.8Φ_N), region III (0.8Φ_N–1.1Φ_N), and region IV (1.1Φ_N–1.45Φ_N). Figure 5(a) presents vibration energy trend versus flow rate at y-direction of different sensors. Vibration energy at sensor 2 (slope volute outlet) is much larger than that at other sensors at variable flow rates. Meanwhile, sensor 1 and sensor 7 are in symmetrical position, so vibration energy trends and values of two sensors are quite similar. When model pump operates in region I (0–0.3Φ_N), according to head curve, rotating stall phenomenon occurs in interior impeller channels causing partial channels to be blocked. The stall cell transfers from one impeller channel to the adjacent channel forming unsteady characteristic leading to vibration energy increasing rapidly. Especially at sensor 2, vibration energy has about an increment of 3 dB. When model pump works in region II, from 0.8Φ_N to 0.3Φ_N, partial flow separates from blade suction side with flow rate decreasing. The separated flow structure leads to vibration energy at y-direction increasing gradually. Vibration energy has an increment of 1.28 dB at sensor 2 and about 1.5 dB at sensors 1 and 7. At sensors 3, 5, and 6, the increment almost reaches 2 dB. In region III, flow field interior impeller channels is relatively uniform, and separated flow structure does not occur. But from 1.1Φ_N to 0.8Φ_N, flow pattern around slope volute tongue may change remarkably. According to our previous work, at 1.1Φ_N, fluid flows into diffusion section smoothly; however, at 0.8Φ_N, partial fluid flows back into volute striking with volute tongue intensively. And the backflow structure has an evident impact on vibration energy. From 1.1Φ_N to 0.95Φ_N, at sensors 2 and 3, vibration energy increases about 1.45 dB. After that vibration energy decreases rapidly. In region IV, with flow rate increasing, vortex sheds from blade pressure side due to fluid striking effect, which also causes vibration energy increasing obviously. Particularly at sensor 2, the increment reaches 1.9 dB. Figure 5(b) presents total vibration energy trends of triaxial accelerometers at various flow rates. Some discrepancies can be found compared with vibration characteristics in Figure 5(a). In region II, from 0.7Φ_N to 0.3Φ_N, vibration energy almost keeps unchanged, which is not affected by the separated flow structure. And around best efficiency point 1.0Φ_N, vibration energy trend falls to a local minimum; after that it rises again.

4.2. Results at Cavitation Condition. Cavitation usually has a great influence on performance of model pump, and Figure 6 presents total delivery head coefficient versus cavitation number from flow rate 0.9Φ_N to 1.4Φ_N. At higher value of cavitation number, total delivery head of model pump almost remains substantially constant. With the decreasing of σ, the available NPSH is insufficient, which results in cavitation starting to develop interior model pump. The total delivery head falls to 3% drop point, where cavitation is considered full developed as seen in the block dots in Figure 6 [18]. So the 3% head drop point was usually defined as critical net positive suction head (NPSH$_c$). Limited by the experimental system, NPSH$_c$ at 0.9Φ_N could not be attained:

$$\text{NPSH} = \frac{P_1 - P_v}{\rho g} + \frac{v_1^2}{2g}, \tag{4}$$

where P_1 is the absolute static pressure at pump inlet, P_v is the vapor pressure, and v_1 is the absolute velocity at pump inlet.

Cavitation number is usually defined as in

$$\sigma = \frac{\text{NPSH}}{H}. \tag{5}$$

Because of the physical nature of cavitation, high frequency signals would be excited during collapse process of cavitation bubbles. Vibration signals in 0–10 Hz band were filtered [19]. So vibration characteristics in 10 Hz–25 kHz band were investigated. Figure 7 shows vibration spectra at y-direction of sensor 3 at cavitation and noncavitation conditions when model pump operates at designed flow rate. At full developed cavitation condition, the amplitudes of broad-band vibration signals increase significantly, especially within higher frequency range. To analyze the impact of cavitation process on vibration signals, vibration spectra were divided into four different frequency bands, 10–500 Hz, 0.5–5 kHz, 5–10 kHz, and 10–25 kHz.

Figure 8 presents RMS trends in four frequency bands versus cavitation number when model pump works at designed flow rate. In 10–500 Hz and 0.5–5 kHz frequency bands, vibration energy trends almost keep constant at higher net positive suction head. However, in 5–10 kHz and 10–25 kHz bands, vibration energy first increases slightly from cavitation numbers 1.48 to 0.58. And in 10–25 kHz band, vibration level has about an average increment of 2–4 dB at different sensors except sensor 5, which increases about 6.5 dB. After that, with cavitation number decreasing further, vibration energy increases rapidly.

Meanwhile, total delivery head reaches 1.6% drop point. So cavitation number $\sigma = 0.58$ could be defined as cavitation inception point. With cavitation number decreasing, the influence of cavitation process on vibration energy in different frequency bands is not similar. Cavitation numbers from 0.58 to 0.17, RMS values in 10–500 Hz, 5–10 kHz, and 10–25 kHz bands, have the same trend. Vibration energy first rises to a local maximum at $\sigma = 0.26$, then falls to a local minimum around $\sigma = 0.21$, which is much smaller than critical net positive suction head, and finally increases again. Cavitation number from 0.58 to 0.26, vibration energy has about an increment of 1–3 dB in 10–500 Hz frequency band.

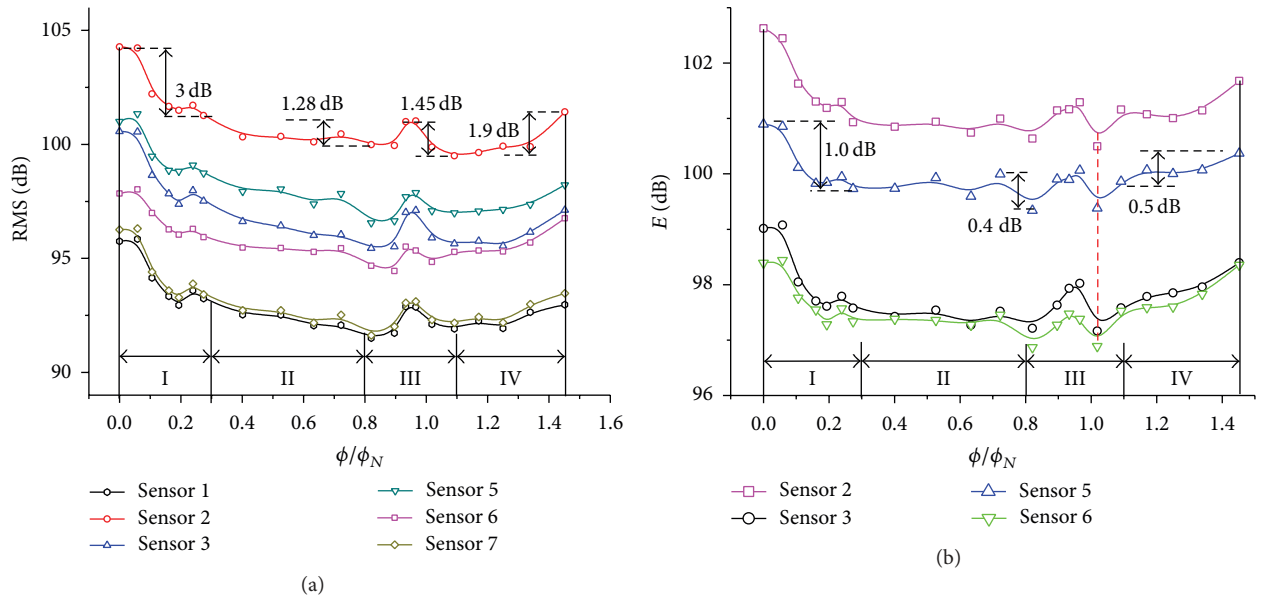

FIGURE 5: (a) Vibration energy trend versus flow rate at y-direction; (b) total vibration energy trend.

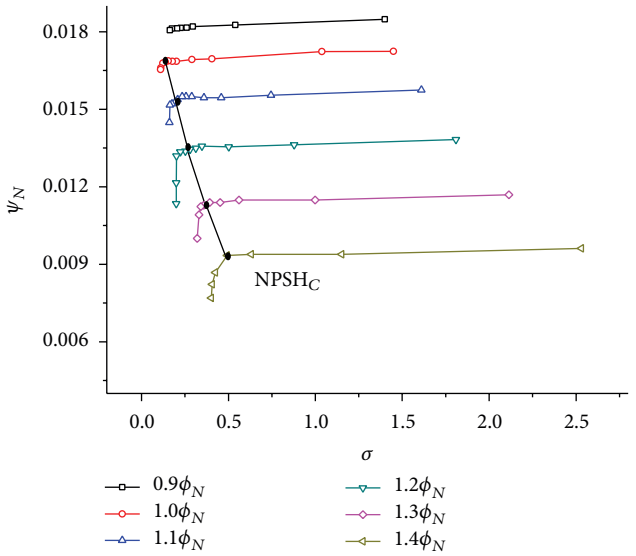

FIGURE 6: Total delivery head coefficient versus cavitation number.

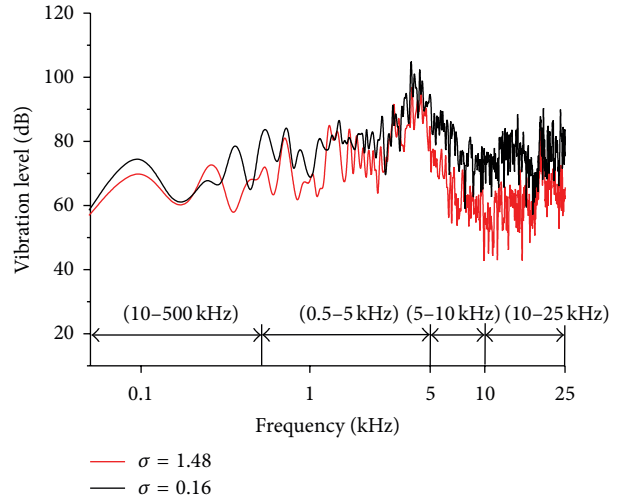

FIGURE 7: Vibration spectra at y-direction of sensor 3 at cavitation (thick line) and noncavitation condition (thin line).

But in high frequency band 10–25 kHz, vibration energy nearly has an increment of 9 dB at variable sensors, which is adequate to detect full developed cavitation status in centrifugal pump. However, in 0.5–5 kHz band, vibration energy at different sensors increases continuously except at sensor 2.

From comparison of vibration energy in different frequency bands, it is found that some differences exist in vibration energy trend during development process of cavitation. At the beginning, with net positive suction head decreasing, some small bubbles develop near blade leading edge. Affected by the occurring of cavitation bubbles, σ, from 1.48 to 0.58, total delivery head of model pump descends slightly. The small bubbles travel towards blade exit and collapse at high pressure region. According to theoretical analysis, it is known that high frequency noises would be excited during collapse process of small bubbles, which have a significant effect on vibration energy in high frequency bands. As presented in Figure 7, vibration energy in 5–10 kHz and 10–25 kHz bands increases along with cavitation number decreasing. But the emitted high frequency noises almost have little influence on vibration energy in 10–500 Hz and 0.5–5 kHz bands. So it is concluded that high vibration signals are much more effective in detecting incipient cavitation in centrifugal pump. With cavitation number decreasing, from 0.58 to 0.26, cavitation region near suction side of blade inlet expands causing vibration in different frequency bands increasing to a local

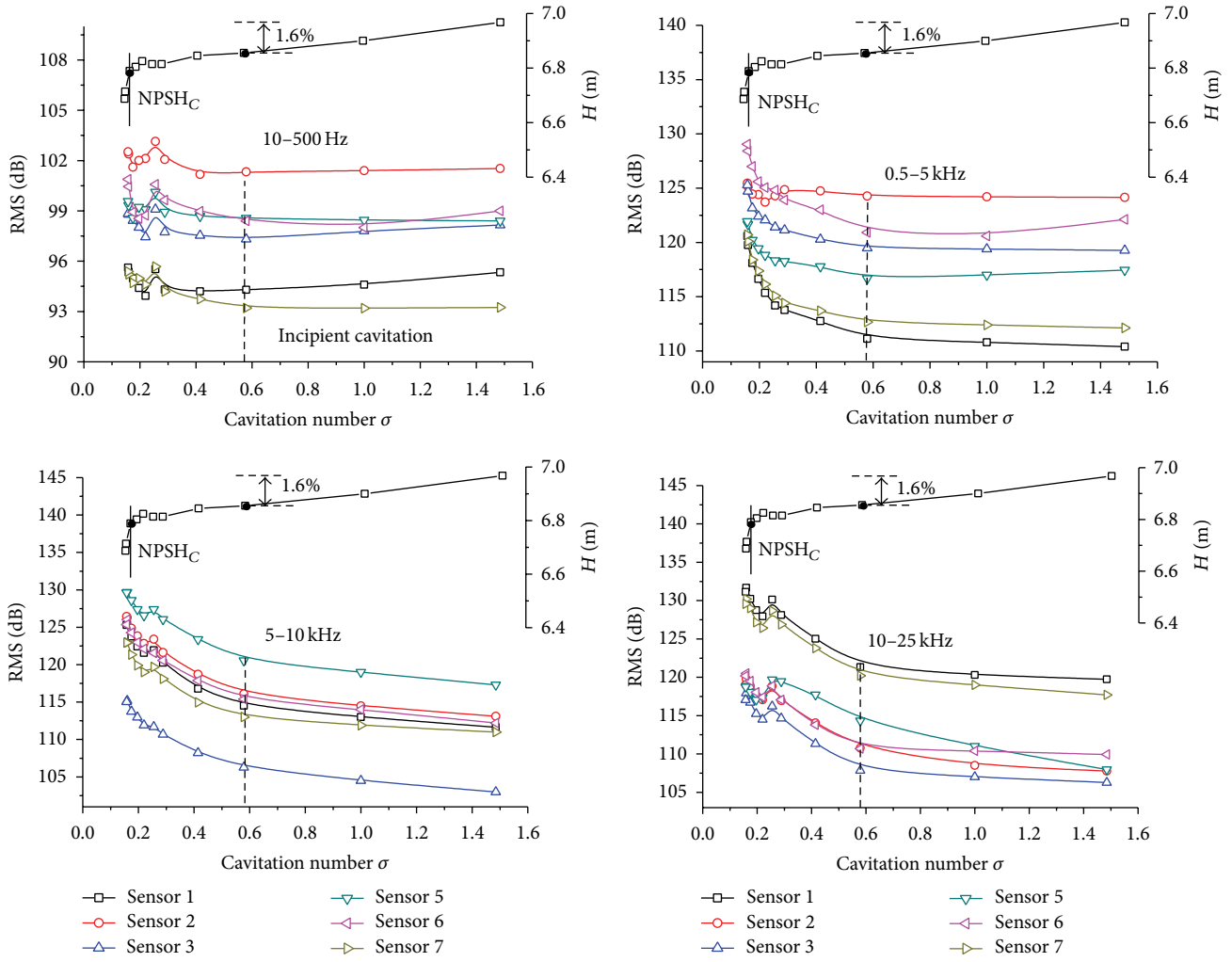

Figure 8: RMS value trends in different frequency bands versus cavitation number at y-direction.

maximum. When cavitation number was reduced further, from 0.26 to 0.21, the type of cavitation changes from cloud to bubble cavitation-macroscopic bubbles [7]. Vibration energy in 10–500 Hz, 5–10 kHz, and 10–25 kHz bands decreases dramatically and reaches a local minimum. The reason probably lies in the fact that flow field interior impeller is in a state of two-phase bubbly flow region. The emitted noises during collapse of bubbles would be attenuated obviously because of the highly compressible two-phase flow. However, vibration energy trends in 0.5–5 kHz do not follow the rule for all the sensors, which increase with cavitation number decreasing except at sensor 2. With cavitation number continuously decreasing, $\sigma < 0.21$, cavitation region on blade suction side expands towards both blade exit and middle of blade channel. A significant free surface between liquid and vapor exists; thus, the compressibility of this fluid status is much smaller. So noises emitted from collapse of cavitation bubbles are less weak. Vibration energy in different frequency bands increases rapidly again at small cavitation number.

Figure 9 shows total vibration energy of triaxial accelerometers in different frequency bands versus cavitation number when model pump works at nominal flow rate. It is found that vibration energy trends are similar to that at y-direction. High frequency signals are much more sensitive to incipient cavitation. When incipient cavitation occurs, vibration energy increases simultaneously. Cavitation numbers from 0.26 to 0.21 rapidly drop in vibration energy trends in 10–500 Hz, 5–10 kHz, and 10–25 kHz bands, which can also be observed due to the high compressibility of two-phase fluid.

To analyze vibration energy trends at different flow rates, Figure 10 presents total vibration energy trends of sensor 3. It can be discovered that the effect of cavitation on vibration at variable flow rates differs quite a lot. Due to the nature of cavitation, it is well accepted that high frequency signals would be emitted during collapse of cavitation bubbles [20]. Generally, cavitation noise signals above 1 kHz were analyzed in most of the reported researches. According to McNulty [12], low frequency signals below 1 kHz were filtered due to the high level of shaft and blade passing frequency noises. In consequence, cavitation noises in low frequency band were rarely investigated. However, according to the results of

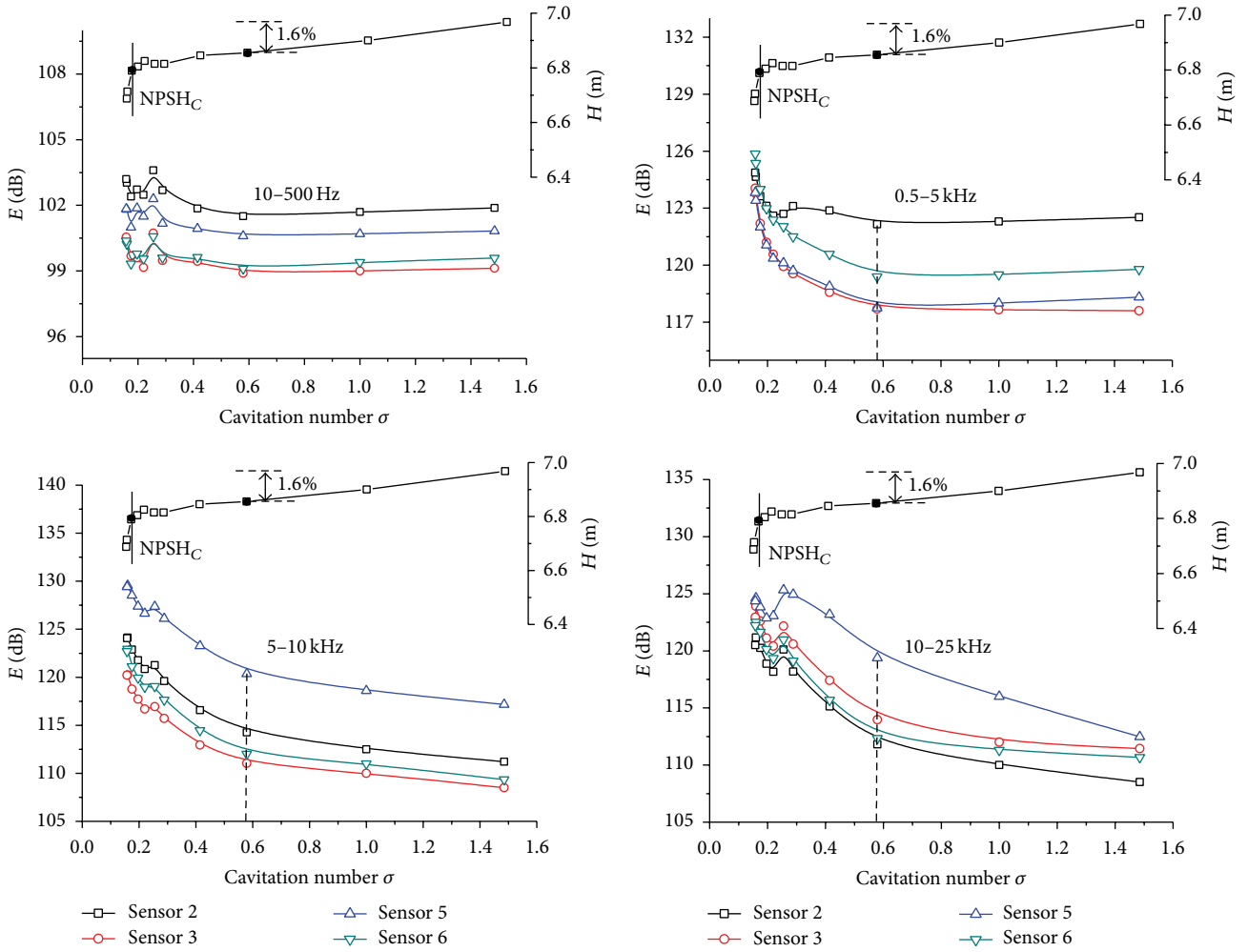

Figure 9: Total vibration energy of triaxial accelerometers in different frequency bands versus cavitation number.

Figures 7 and 8, cavitation process has a significant impact on vibration signals in low frequency band. So it is essential to have an overall understanding of vibration noises in low frequency band at different flow rates. In 10–500 Hz band, at the beginning, vibration energy trends almost keep constant with cavitation number decreasing. When incipient cavitation, the square point in Figure 10, was achieved, vibration energy starts to increase steeply and arrives at a local maximum. At $1.0\Phi_N$, cavitation number σ from 0.58 to 0.26, vibration level increases 1.83 dB. The increments of vibration level from cavitation inception point to local maximum point rise along with flow rates increasing. At $1.4\Phi_N$, the increment reaches 3.83 dB, which is enough for detecting cavitation in centrifugal pump. Then it decreases drastically and finally increases again at small cavitation number. In 0.5–5 kHz band, vibration energy at different flow rates almost increases continuously with the development process of cavitation and steeply drop phenomenon in vibration level curves was not observed. At $1.0\Phi_N$, σ from 0.58 to 0.16, vibration level nearly increases 6.3 dB. And at higher flow rate $1.4\Phi_N$, σ from 1.5 to 0.4, it has an increment of 9.5 dB. In 5–10 kHz and 10–25 kHz bands, vibration energy trends at $1.0\Phi_N$ and $1.1\Phi_N$ are similar to that in 10–500 Hz band. However, at higher flow rates, vibration trends do not follow the rule. The vibration energy starts to increase with development of cavitation process until it reaches a local maximum value; then, at full developed cavitation condition vibration energy starts to decrease. But another increase in vibration level does not occur. The reason probably can be contributed to the increasing number and volume of cavitation bubbles. At high flow rates, the number and size of cavitation bubbles increase much more rapidly than those at low flow rates. And the development process of cavitation is rather intensive, so single phase fluid status no longer exists. When cavitation bubbles are abundant, two-phase fluid status interior impellers are formed. The emitted noises during collapse of bubbles are attenuated [7]. So another increase in vibration energy could not be found.

From the above analysis, it is found that a closed correlation exists between vibration energy and development process of cavitation. From Figures 8 and 9, it is clear that vibration energy was affected much earlier before 3% head drop point. So to detect cavitation in centrifugal pump, determination of head drop usually is not effective and sufficient. It is necessary to clarify the difference of critical

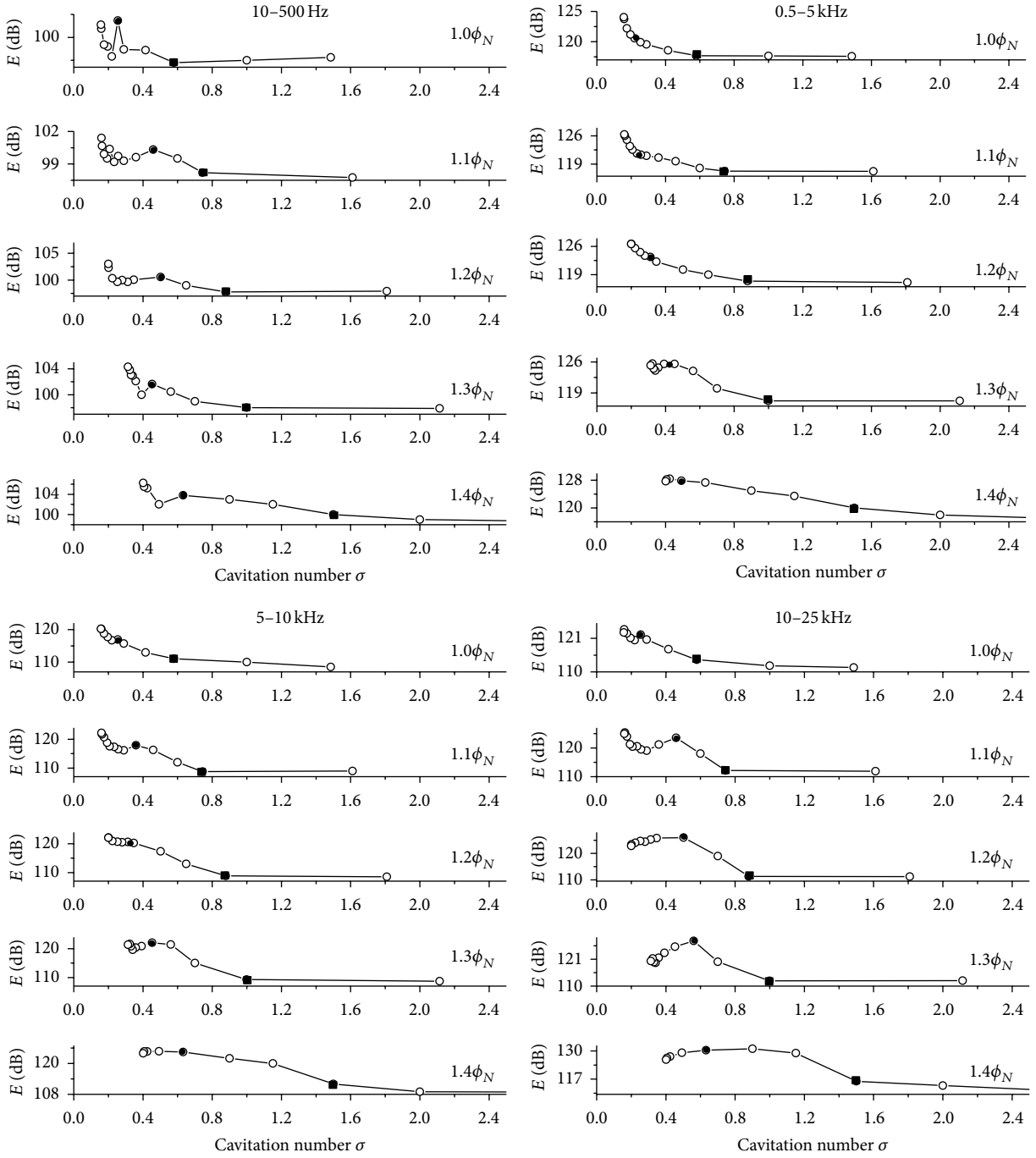

Figure 10: Total vibration energy at sensor 3 in different frequency bands versus cavitation number.

point from vibration level and 3% head drop. The cavitation inception point was chosen where vibration level increases steeply as seen in the square points in Figure 10. And the critical point of vibration level was defined where vibration energy trend achieves a local maximum point or a change in slope (steep increase in slope) as seen in the black dots in Figure 10. Severe cavitation erosion danger may exist at the local maximum point. Critical points extracted from vibration energy trend in different frequency bands and 3% head drop at variable flow rates were presented in Figure 11. It is clear that critical point obtained from 3% head drop increases along with flow rates rising. Also, it is noted that the difference between critical points based on vibration level at different frequency bands is fairly huge, which indicates that the influence of development process of cavitation on different frequency signals is not similar. Critical points obtained from vibration level are much larger than that from 3% head drop at different flow rates. So it is proved that full developed cavitation is much earlier than that reflected in head curve of model pump.

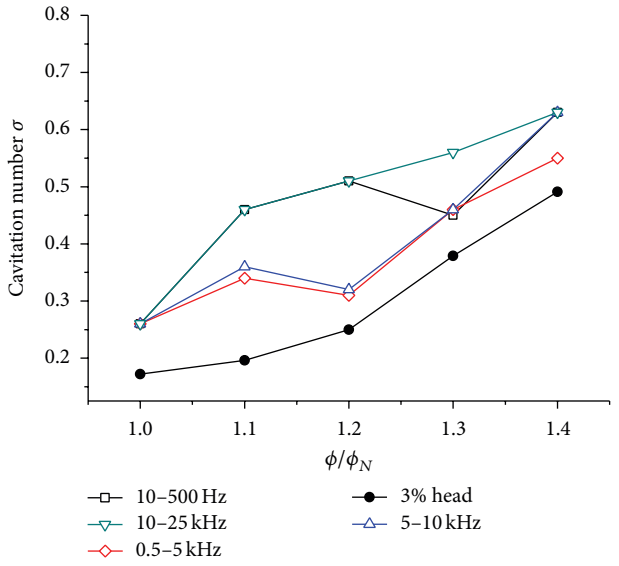

Figure 11: Comparison of critical point based on total vibration energy and 3% head drop at sensor 3.

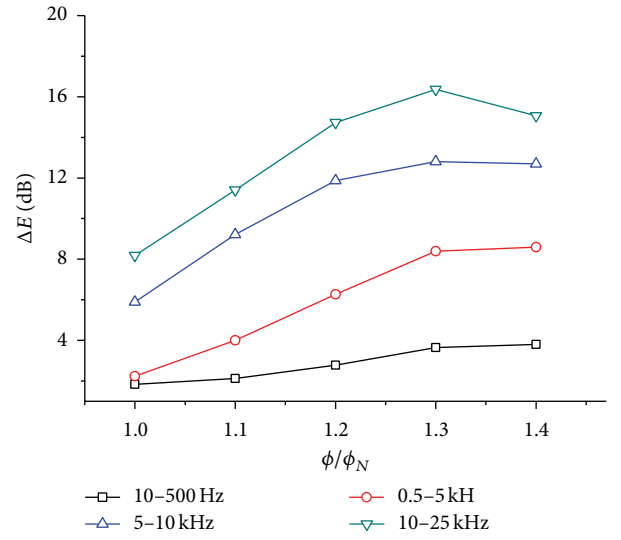

Figure 12: Increment of vibration level from cavitation inception to critical point.

To detect cavitation in centrifugal pump, the most common method, 3% drop in head curve, was used. However, from the above results, it is known that cavitation occurs much earlier than that obtained from 3% head drop. So vibration measurement can supply an effective solution. At sensor 3, increments of total vibration energy in different frequency bands from cavitation inception to critical point are presented in Figure 12. The increments at nominal flow rate are much smaller than that at high flow rate. In high frequency bands 5–10 kHz and 10–25 kHz, the increments are much larger than that at low frequency bands. In 10–25 kHz band, the increment reaches 8.2 dB at designed flow rate and 16.4 dB at $1.3\Phi_N$ flow rate, which are adequate for detecting full developed cavitation. So it is concluded that high frequency signals can be used to detect cavitation effectively in centrifugal pump.

5. Conclusions

In this paper, vibration characteristics of a centrifugal pump with slope volute were investigated. At noncavitation condition, vibration energy trend in 10–500 Hz band versus flow rate was analyzed. A closed relationship between flow structure and vibration energy could be found. At off-design conditions, especially low flow rates, vibration energy rises rapidly along with the rotating stall occurring. And at y-direction of sensor 2, flow rate from $0.3\Phi_N$ to shutoff condition, vibration energy has about an increment of 3 dB. At cavitation condition, vibration signals were divided into four typical frequency bands to analyze vibration characteristics. It is clear that low frequency signals are affected by cavitation process significantly. At $1.0\Phi_N$, total vibration level increases about 1.83 dB from incipient cavitation point to critical point. And critical points based on vibration in variable frequency bands are much larger than that from 3% head drop. In particular, for signals in 10–25 kHz band, high frequency signals are more sensitive to onset of cavitation. From cavitation inception to critical point, vibration level increases rapidly, and the increment is enough to detect cavitation in centrifugal pump. So it is concluded that vibration signals can be used to monitor full developed cavitation, which can effectively replace the 3% head drop means.

Conflict of Interests

The authors declare that there is no conflict of interests regarding the publication of this paper.

Acknowledgments

The authors gratefully acknowledge the financial support of National Natural Science Foundation of China (51206063, 51106066), a Project Funded by the Priority Academic Program Development of Jiangsu Higher Education Institutions (PAPD), and the Research and Innovation Project for College Graduates of Jiangsu Province (KYLX_1036).

References

[1] M. Dular, B. Bachert, B. Stoffel, and B. Širok, "Relationship between cavitation structures and cavitation damage," *Wear*, vol. 257, no. 11, pp. 1176–1184, 2004.

[2] C. E. Brennen, *Cavitation and Bubble Dynamics*, Oxford University Press, New York, NY, USA, 1994.

[3] R. Balasubramanian, S. Bradshaw, and E. Sabini, "Influence of impeller leading edge profiles on cavitation and suction performance," in *Proceedings of the 27th International Pump Users Symposium*, pp. 1–11, Houston, Tex, USA, September 2011.

[4] M. Čudina, "Detection of cavitation phenomenon in a centrifugal pump using audible sound," *Mechanical Systems and Signal Processing*, vol. 17, no. 6, pp. 1335–1347, 2003.

[5] Y. Wang, H. L. Liu, S. Q. Yuan, D. Liu, and J. Wang, "Characteristics of cavitation vibration and noise in centrifugal pumps with different vane wrap angles," *Journal of Drainage and Irrigation Machinery Engineering*, vol. 31, no. 5, pp. 390–400, 2013.

[6] S. Christopher and S. Kumaraswamy, "Identification of critical net positive suction head from noise and vibration in a radial flow pump for different leading edge profiles of the vane," *Journal of Fluids Engineering*, vol. 135, no. 12, Article ID 121301, 2013.

[7] T. Rus, M. Dular, B. Širok, M. Hočevar, and I. Kern, "An investigation of the relationship between acoustic emission, vibration, noise, and cavitation structures on a Kaplan turbine," *Journal of Fluids Engineering*, vol. 129, no. 9, pp. 1112–1122, 2007.

[8] M. Čudina and J. Prezelj, "Detection of cavitation in operation of kinetic pumps. Use of discrete frequency tone in audible spectra," *Applied Acoustics*, vol. 70, no. 4, pp. 540–546, 2009.

[9] M. Chudina, "Noise as an indicator of cavitation in a centrifugal pump," *Acoustical Physics*, vol. 49, no. 4, pp. 463–474, 2003.

[10] Y. Y. Ni, S. Q. Yuan, Z. Y. Pan, and J. Yuan, "Detection of cavitation in centrifugal pump by vibration methods," *Chinese Journal of Mechanical Engineering*, vol. 21, no. 5, pp. 46–49, 2008.

[11] I. S. Pearsall, "Acoustic detection of cavitation," in *Proceedings of the Institution of Mechanical Engineers Conference (MECH '66)*, vol. 181 of *Part 3A, paper no.14.1966*, 1966.

[12] P. J. McNulty and I. S. Pearsall, "Cavitation inception in pumps," *Journal of Fluids Engineering*, vol. 104, no. 1, pp. 99–104, 1982.

[13] M. G. Yang, N. Zhang, Z. Li, and B. Gao, "Optimal design of centrifugal pump with tilt volute based on CFD," *Journal of Jiangsu University (Natural Science Edition)*, vol. 34, no. 1, pp. 28–32, 2013.

[14] N. Zhang, M. G. Yang, B. Gao et al., "Unsteady phenomena induced pressure pulsation and radial load in a centrifugal pump with slope volute," in *Proceedings of the ASME Fluids Engineering Division Summer Meeting (FEDSM '13)*, Incline Village, Nev, USA, July 2013.

[15] T. Minggao, W. Yong, L. Houlin, W. Xianfang, and W. Kai, "Effects of number of blades on flow induced vibration and noise of centrifugal pumps," *Journal of Drainage and Irrigation Machinery Engineering*, vol. 30, no. 2, pp. 131–135, 2012.

[16] A. Lucius and G. Brenner, "Numerical simulation and evaluation of velocity fluctuations during rotating stall of a centrifugal pump," *Journal of Fluids Engineering*, vol. 133, no. 8, Article ID 081102, 2011.

[17] X. Escaler, E. Egusquiza, M. Farhat, F. Avellan, and M. Coussirat, "Detection of cavitation in hydraulic turbines," *Mechanical Systems and Signal Processing*, vol. 20, no. 4, pp. 983–1007, 2006.

[18] O. Coutier-Delgosha, R. Fortes-Patella, J. L. Reboud, M. Hofmann, and B. Stoffel, "Experimental and numerical studies in a centrifugal pump with two-dimensional curved blades in cavitating condition," *Journal of Fluids Engineering*, vol. 125, no. 6, pp. 970–978, 2003.

[19] S. Lahdelma and E. K. Juuso, "Vibration analysis of cavitation in Kaplan water turbines," in *Proceedings of the 17th IFAC World Congress*, pp. 13420–13425, Seoul, Republic of Korea, July 2008.

[20] M. R. Nasiri, M. J. Mahjoob, and H. Vahid-Alizadeh, "Vibration signature analysis for detecting cavitation in centrifugal pumps using neural networks," in *Proceedings of the IEEE International Conference on Mechatronics (ICM '11)*, pp. 632–635, Istanbul, Turky, April 2011.